

Ultrafast electron dynamics and cubic optical nonlinearity of free standing thin film of double walled carbon nanotubes

N. Kamaraju^{1,2}, Sunil Kumar^{1,2}, B. Karthikeyan^{1,2},
 Alexander Moravsky³, R. O. Loutfy³ and A.K. Sood^{1,2*}

¹*Center for Ultrafast Laser Applications (CULA),
 Indian Institute of Science, Bangalore - 560 012, India*

²*Department of Physics, Indian Institute of Science, Bangalore - 560 012, India and*

³*Materials and Electrochemical Research Corporation, Tucson, AZ, USA*

(Dated: June 17, 2008)

Abstract

Ultrafast degenerate pump-probe experiments performed on a free standing film of double walled carbon nanotubes near the first metallic transition energy of outer tube show ultrafast ($97\ fs$) photobleaching followed by a photo-induced absorption with a slow relaxation of $1.8\ ps$. Femtosecond closed and open aperture z-scan experiments carried out at the same excitation energy show saturation absorption and negative cubic nonlinearity. From these measurements, real and imaginary part of the third order nonlinear susceptibility are estimated to be $\text{Re}(\chi^{(3)}) \sim -2.2 \times 10^{-9}\ esu$ and $\text{Im}(\chi^{(3)}) \sim 1.1 \times 10^{-11}\ esu$.

PACS numbers: 78.47.+p: Time-resolved optical spectroscopies and other ultrafast optical measurements in condensed matter, 42.65.An: Optical susceptibility and hyper polarizability and 78.67.ch: optical properties of nanotubes

* Electronic mail: asood@physics.iisc.ernet.in

Hollow cylinders made by folding graphene sheet named as Carbon nanotubes (CNTs), have attracted intensive research due to their fascinating physical properties with possible applications such as in mechanics,¹ flow transducers,² nanoelectronics^{3,4}, and nonlinear optics.^{5,6,7} One dimensional nature of delocalized π -electron cloud along the tube axis,^{8,9} make CNTs the most promising material with large and ultrafast electronic third order susceptibility¹⁰ to be utilized in exciting applications like optical terahertz (THz) switching and passive modelocking. Femtosecond time resolved photoinduced studies on single walled nanotubes (SWNT)^{11,12,13,14,15,16,17,18,19} reveal that the excitons are the primary photoexcitations in semiconducting-SWNT (s-SWNT) whereas free carriers are photoexcited in metallic-SWNT (m-SWNT). These studies indicate that the photoinduced response changes from fast (≤ 5 ps) to slow (30 ps) when the SWNTs are dispersed in a liquid from their bundled state. The relaxation mechanisms are different in metallic and semiconducting nanotubes. Electron-electron and electron-phonon interactions contribute to fast and slow components, respectively, in m-SWNT^{12,20,21}. On the other hand, in s-SWNT intra-band carrier relaxation and inter-band carrier recombination lead to fast and slow relaxations respectively^{12,17,18,19}. Environmental effects and defects also play a major role in these relaxation processes.^{12,22} Chen *et al.*²³, measured the $\text{Im}(\chi^{(3)}) \sim 10^{-10}$ esu whereas Maeda *et al.*¹⁰ reported that $\text{Im}(\chi^{(3)})$ could be as high as 10^{-6} esu in the case of s-SWNT films on a substrate. Recent z-scan measurements²⁴ at 1.57 eV showed $\text{Im}(\chi^{(3)}) = 10^{-9}$ esu and $\text{Re}(\chi^{(3)}) = -4.4 \times 10^{-9}$ esu for SWNT-suspensions (using a surfactant) and $\text{Im}(\chi^{(3)}) = 8 \times 10^{-9}$ esu and $\text{Re}(\chi^{(3)}) = 1.4 \times 10^{-8}$ esu at 0.85 eV for SWNT thin films²⁵. In the case of multi walled carbon nanotubes (MWNT) grown on a quartz substrate²⁶, the values are $\text{Im}(\chi^{(3)}) = -1.6 \times 10^{-11}$ esu and $\text{Re}(\chi^{(3)}) = -1.7 \times 10^{-11}$ esu, and photobleaching decay time of ~ 2 ps was reported. As compared to SWNT and MWNT, double walled carbon nanotubes (DWNT) have not been investigated for their nonlinear properties, except the work of Nakamura *et al.*,²⁷ where pump-probe studies show photo bleaching with biexponential relaxation for DWNT suspensions. The shortest decay time (400 fs) of photobleaching was attributed to carrier relaxation between inner and outer tubes and the slow component (4 ps) was ascribed to the recombination of electrons and holes at the bottom of the bands. Except this study, there has been no other study to our knowledge on DWNT. In this letter, we report degenerate Pump-Probe (PP) measurements and femtosecond z-scan experiments (both closed aperture (CA) and open aperture (OA)) on unsupported film of

DWNT. We show that the $\text{Im}(\chi^{(3)})$ is two orders of magnitude smaller compared to that of SWNT aqueous suspensions²⁴ whereas the $\text{Re}(\chi^3)$ is of the same order of magnitude.

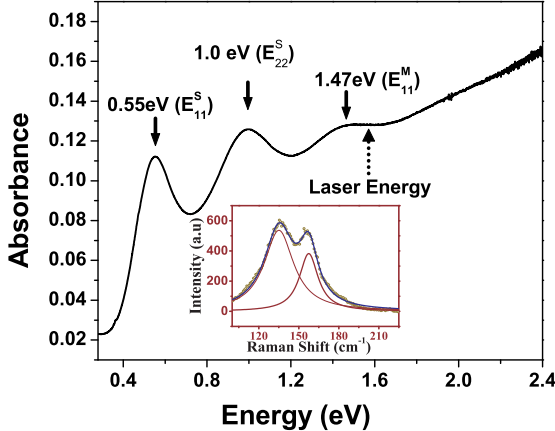


FIG. 1: Optical absorption spectrum of double walled carbon nanotube film. E_{11}^S and E_{22}^S are the first and second interband transition energies of the semiconducting nanotubes and E_{11}^M is the first transition energy of metallic tubes. Dotted arrow shows the energy where degenerate PP and z-scan measurements were done. Inset shows RBM modes at 135 cm^{-1} and 157 cm^{-1} corresponding to the average diameter of 1.97 nm and 1.65 nm respectively of the outer tubes.

DWNT films of thickness 200 nm (measured using Atomic Force Microscopy (AFM)) were prepared as reported elsewhere²⁸ and characterized by Raman spectroscopy (using Ar ion laser at 2.41 eV) and optical absorption (Bruker FT-IR) spectroscopy. Inset of Fig. 1 shows radial breathing modes (RBM) of DWNT at 135 cm^{-1} and 157 cm^{-1} , corresponding to the outer tube average diameters of 1.97 nm and 1.65 nm , respectively. Fig. 1 displays the optical absorption spectrum of the DWNT film showing three bands at 0.55 eV , 1.0 eV and 1.47 eV corresponding to E_{11}^S , E_{22}^S and E_{11}^M electronic transitions of the outer tube of diameter 1.97 nm , as suggested by the theoretical calculations.²⁹ The dotted arrow in Fig. 1 marks the laser photon energy, E_L of 1.57 eV used in all our experiments which is very close to E_{11}^M . The refractive index, n_0 of the DWNT film is 3.6 at 1.57 eV as calculated from its absorption and transmission measurements using Fresnel's relation between reflection coefficient and extinction coefficient.³⁰

The output from Ti:Sapphire Regenerative femtosecond amplifier (50 fs, 1.57 eV , 1 KHz Spitfire, Spectra Physics) was used for both z-scan and the degenerate PP experiments.

At the sample point, the cross-correlation of pump and probe pulses was measured to be 75 fs (FWHM) using a thin BBO crystal. The pump pulse was delayed in time using the computer controlled motorized translation stage (XPS Motion controller, Newport). The change in the probe transmission due to the presence of the pump was monitored using two Si-PIN diodes (one for the reference beam and the other for the probe beam interacting with the pump) with the standard lock-in detection (pump beam was chopped at 139 Hz). The probe intensity was kept at 58 MW/cm^2 in all the experiments and the pump intensity was maintained at 1.5 GW/cm^2 , 1.0 GW/cm^2 , 556 MW/cm^2 and 303 MW/cm^2 for intensity dependent PP studies. All these measurements were performed with pump and probe polarizations perpendicular to each other to avoid coherent artifacts³². In the femtosecond z-scan experiments, the intensity was varied from 150 MW/cm^2 to 9.4 GW/cm^2 . The pulse from the amplifier was found to be broadened to 80 fs near the sample point in z-scan experiments. For the CA z-scan, an aperture of 1 mm size was kept in front of the detector whereas for OA z-scan, all the transmitted light was collected.

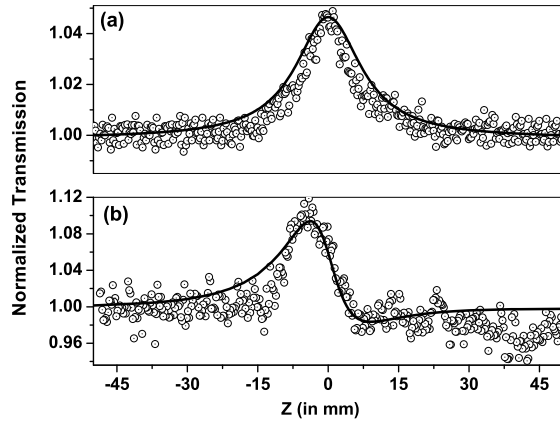


FIG. 2: Normalized transmittance data (open circles) in (a) OA z-scan and (b) CA z-scan (aperture linear transmittance = 0.12). Theoretical fit (solid line) is obtained with $\beta_0 = 1.4 \times 10^{-8} \text{ cm/W}$, $I_s = 13 \text{ GW/cm}^2$ and $\gamma \sim -2.6 \times 10^{-11} \text{ cm}^2/\text{W}$.

The femtosecond OA and CA z-scan experiments performed at the same excitation energy (1.57 eV) reveal saturation absorption and negative nonlinearity as shown in Fig. 2 by open circles. Using our modified²⁴ approach to analyze z-scan data, both the OA and CA z-scans were fitted (shown as solid lines in Fig. 2) with a consistent set of parameters,

$\gamma = -2.6 \times 10^{-11} \text{ cm}^2/\text{W}$, $\beta_0 = 1.4 \times 10^{-8} \text{ cm}/\text{W}$ and $I_s = 13 \text{ GW/cm}^2$. Here, γ is the nonlinear refraction coefficient, β_0 is the two photon absorption (TPA) coefficient and I_s is the saturation intensity. The third order nonlinear susceptibility was calculated using³¹ $\text{Im}(\chi^{(3)}) = \frac{6.6 \times 10^{-23} c^2 n_0^2 \beta_0 (\text{in cm}/\text{W})}{96 \pi^2 E_L}$ and $\text{Re}(\chi^{(3)}) = \frac{10^{-7} c n_0^2 \gamma (\text{in cm}^2/\text{W})}{480 \pi^2}$, where c is the velocity of the light in vacuum. The measured values are $\text{Im}(\chi^{(3)}) = 1.1 \times 10^{-11} \text{ esu}$ and $\text{Re}(\chi^{(3)}) = -2.2 \times 10^{-9} \text{ esu}$. It can be seen that as compared to SWNT suspensions²⁴, $\text{Im}(\chi^{(3)})$ is two orders of magnitude smaller whereas the $\text{Re}(\chi^{(3)})$ is of the same order of magnitude.

Degenerate PP data using four different pump intensities is shown in Fig. 3. The initial decay corresponds to photobleaching (PB) and the latter part corresponds to photo-induced absorption (PA). The inset of Fig. 3 shows PA part of differential transmission data (normalized to its PB peak height) for three values of the pump intensities, 303 MW/cm^2 , 556 MW/cm^2 and 1.0 GW/cm^2 . The data for the pump intensity of 556 MW/cm^2 overlaps with that of 303 MW/cm^2 and hence is not shown. The time-dependent photo absorption is fitted with a monoexponential function (shown as solid line in the inset) with a time constant of 1.8 ps for the pump intensities 303 MW/cm^2 and 1.0 GW/cm^2 . It can be seen that the PA is negligible for pump intensity of 1.5 GW/cm^2 and was not analyzed. On the other hand, PB can be resolved for pump intensity of 1.5 GW/cm^2 . The PB data for this pump intensity is fitted with the convolution of the cross-correlation of the pump and probe pulses and a monoexponential function. This yields a time constant of 97 fs. For the lower pump intensities, the decay time decreases below our time resolution (75 fs).

We now offer a plausible explanation of our results. The PB in our experiments at 1.57 eV can only arise from E_{11}^M of m-SWNT since pump and probe energies are nearly resonant with E_{11}^M . The long PA decay time suggests that the excited state absorption could be happening from E_{11}^S excitonic level and not from E_{22}^S excitonic level as earlier PP studies^{11,14} show that PA from E_{22}^S is very fast ($\sim 200 \text{ fs}$). Therefore, the PA will dominantly arise from s-SWNT (transition from excitonic level E_{11}^S to E_{33}^S). Further, PA at 1.57 eV can also arise from m-SWNT (transition from E_{11}^M to E_{33}^M). At higher intensities, larger number of charge carriers are produced which will destroy the excitons in semiconducting tubes. This can result in the decrease of the PA associated with the s-SWNT.

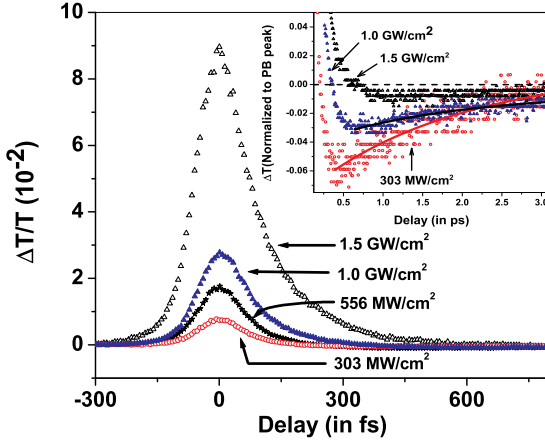


FIG. 3: (colour online) Pump intensity dependent $\Delta T/T$ where the probe intensity is kept at 58 MW/cm^2 . The inset shows PA part of differential transmission data (normalized to its PB peak height) for three values of the pump intensities, 303 MW/cm^2 , 556 MW/cm^2 and 1.0 GW/cm^2 . It can be seen from the inset that the PA is almost negligible for the highest pump intensity. Solid lines are the single exponential decay fit to the data with the time constant of 1.8 ps.

We have also estimated $\text{Im}(\chi^{(3)})$ from PP studies as follows¹⁰.

$$\text{Im}(\chi^{(3)}) = \frac{\varepsilon_0 c^2 n_0^2}{3\omega I_{\text{pump}} \Delta\alpha_0(\tau = 0)} \quad (1)$$

where

$$\Delta\alpha_0(\tau = 0) = \frac{-\alpha_{\text{pump}} \ln \left[\frac{\Delta T}{T}(\tau = 0) + 1 \right]}{1 - e^{-\alpha_{\text{pump}} L_s}} \quad (2)$$

Here, α_{pump} is the linear absorption coefficient of the sample for the pump beam, $\Delta\alpha_0(t)$ is the absorption change of the probe beam when the pump and probe have zero delay ($\tau = 0$), L_s is the sample thickness, ε_0 is the permittivity of vacuum, λ is the wavelength of the light and I_{pump} is the pump intensity. Using measured $\alpha_{\text{pump}} = 6405 \text{ cm}^{-1}$ and $L_s = 200 \text{ nm}$, we get $\beta_0 = 3.9 \times 10^{-8} \text{ cm/W}$ which correspond to $\text{Im}(\chi^{(3)}) = 2.1 \times 10^{-11} \text{ esu}$. This value is found to be independent of the pump intensity and agrees well with the value obtained from our z-scan studies. The ultrafast saturable absorption and large nonlinear third order nonlinearity means that the unsupported film of DWNTs can be used as saturable absorbers in the passive optical regeneration, mode-locking and THz optical switching.

AKS thanks Department of Science and Technology, India, for support.

- ¹ Alan B. Dalton, Steve Collins, Edgar Muoz, Joselito M. Razal1, Von Howard Ebron, John P. Ferraris, Jonathan N. Coleman, Bog G. Kim and Ray H. Baughman, *Nature* **423**, 703 (2003).
- ² S. Ghosh, A.K. Sood and N. Kumar, *Science* **299**, 1042 (2003)
- ³ Philip G. Collins, A. Zettl, Hiroshi Bando, Andreas Thess, R. E. Smalley, *Science* **278**, 100 (1997).
- ⁴ J. A. Misewich, R. Martel, Ph. Avouris, J. C. Tsang, S. Heinze, and J. Tersoff, *Science* **300**, 783 (2003).
- ⁵ Z. X. Jin, X. Sun, G. Q. Xu, S. H. Goh, and W. Ji, *Chem. Phys. Lett.* **318**, 505 (2000).
- ⁶ S. O. Konorov, D. A. Akimov, A. A. Ivanov, M. V. Al'fimov, S. Botti, R. Ciardi, L. De Dominicis, L. S. Asilyan, A. A. Podshivalov, D. A. Sidorov-Biryukov, R. Fantoni and A. M. Zheltikov1, *J. Raman Spectrosc.* **34**, 1018 (2003).
- ⁷ L. Vivien, E. Anglaret, D. Riehl, F. Bacou, C. Journet, C. Goze, M. Andrieux, M. Brunet, F. Lafonta, P. Bernier, F. Hache, *Chem. Phys. Lett.* **307**, 317 (2000).
- ⁸ V.A. Margulis, *J. Phys.: Condens. Matter* **11**, 3065 (1999)
- ⁹ J. S. Lauret, C. Voisin, G. Cassabois, J. Tignon, C. Delalande, Ph. Roussignol, O. Jost and L. Capes *Appl. Phys. Lett.* **85**, 3572 (2004).
- ¹⁰ A. Maeda, S. Matsumoto, H. Kishida, T. Takenobu, Y. Iwasa, M. Shiraishi, M. Ata, and H. Okamoto *Phys. Rev. Lett.* **94**, 047404 (2005).
- ¹¹ O. J. Korovyanko, C.-X. Sheng, Z.V. Vardeny, A.B. Dalton and R.H. Baughman, *Phys. Rev. Lett.* **92**, 017403 (2004)
- ¹² M. Ichida, Y. Hamanaka, H. Kataura, Y. Achiba and A. Nakamura *J. Phys. Soc. Jap.* **73**, 3479 (2004).
- ¹³ C. Manzoni, A. Gambetta, E. Menna, M. Meneghetti, G. Lanzani, and G. Cerullo, *Phys. Rev. Lett.* **94**, 207401 (2005).
- ¹⁴ R. J. Ellingson, C. Engtrakul, M. Jones, M. Samec, G. Rumbles, A. J. Nozik, and M.J. Heben, *Phys. Rev. B* **71**, 115444 (2005).
- ¹⁵ T. Hertel, R. Fasel, and G. Moos, *Appl. Phys. A: Mater. Sci. Process.* **75**, 449 (2002)
- ¹⁶ M. Ichida, Y. Hamanaka, H. Kataura, Y. Achiba, and A. Nakamura, *Physica B* **323**, 237 (2002).

¹⁷ J. S. Lauret, C. Voisin, G. Cassabois, C. Delalande, P. Roussignol, O. Jost, and L. Capes, Phys. Rev. Lett. **90**, 057404 (2003).

¹⁸ G. N. Ostojic, S. Zaric, J. Kono, M. S. Strano, V. C. Moore, R. H. Hauge, and R. E. Smalley, Phys. Rev. Lett. **92**, 117402 (2003).

¹⁹ J. S. Lauret, C. Voisin, G. Cassabois, P. Roussignol, C. Delalande, L. Capes, E. Valentin, A. Filoromo, and O. Jost, Semicond. Sci. Technol. **19**, S486 (2004).

²⁰ T. Hertel and G. Moos, Phys. Rev. Lett **84**, 5002 (2000).

²¹ T. Hertel, A. Hagen, V. Talalaev, K. Arnold, F. Hennrich, M. Kappes, S. Rosenthal, J. McBride, H. Ulbricht and E. Flahaut, Nano Lett. **5**, 511 (2005).

²² J. S. Lauret, C. Voisin, S. Berger, G. Cassabois, C. Delalande, Ph. Roussignol, L. Goux-Capes and A. Filoromo, Phys. Rev. B **72**, 113413 (2005).

²³ Y.C. Chen, N.R. Raravikar, L.S. Schadler, P. M. Ajayan, Y. P. Zhao, T.M. Lu, G.C. Wang, X.C. Zhang Appl. Phys. Lett. **81**, 975 (2002).

²⁴ N. Kamaraju, Sunil Kumar, S. Krishnamurthy, S. Guha, A. K. Sood, C. N. R. Rao, Appl. Phys. Lett. **91**, 251103 (2007).

²⁵ Daisuke Shimamoto, Takaaki Sakurai, Minoru Itoh, Yoong Ahm Kim, Takuya Hayashi, Morinobu Endo and Mauricio Terrones Appl. Phys. Lett. **92**, 081902 (2008).

²⁶ H.I. Elim, W. Ji, G.H. Ma, K. Y. Lim, C. H. sow and H. A. Huan Appl. Phys. Lett. **85**, 1799 (2004).

²⁷ A. Nakamura, T. Tomikawa, M. Watanabe, Y. Hamanaka, Saiti, H. Ago J. Lumi. **119**, 8 (2006).

²⁸ Vikram Gadagkar, Surajit Saha, D. V. S. Muthu, Prabal K. Maiti, Yves Lansac, A. Jagota, Alexander Moravsky, R. O. Loutfy and A. K. Sood, J. Nanoscience and Nanotechnology **7**, 1753 (2007)

²⁹ S. Reich, C. Thomsen, J. Maultzsch, *Carbon nanotubes* (Wiley-VCH Verlag GmbH Co KGaA, Weinheim, 2004), pp. 69-70.

³⁰ J. I. Pankove, *Optical processes in semiconductors* (Dover Publications Inc, New york, 1975), pp. 90-91.

³¹ R A Ganeev, J. Opt. A: Pure Appl. Opt. **7**, 717 (2005).

³² H. Okamoto, S. Matsumoto, A. Maeda, H. Kishida, Y. Iwasa, and T. Takenobu, Phys. Rev. Lett. **96**, 019706 (2006).